High Energy Density Physics 8 (2012) 313–321

Contents lists available at SciVerse ScienceDirect

High Energy Density Physics

journal homepage: www.elsevier.com/locate/hedp

Irradiated interfaces in the Ara OB1, Carina, Eagle Nebula, and Cyg OB2 massive star formation regions

P. Hartigan [a,b,*], J. Palmer [a,b], L.I. Cleeves [b,c]

[a] Physics and Astronomy Dept., Rice University, Houston, TX, USA
[b] NOAO Observatories, USA
[c] Astronomy Dept., University of Michigan, Ann Arbor, MI, USA

ARTICLE INFO

Article history:
Received 24 July 2012
Accepted 29 August 2012
Available online 5 September 2012

Keywords:
Radiation hydrodynamics
Laboratory astrophysics
Astronomical images
Photodissociation regions

ABSTRACT

Regions of massive star formation offer some of the best and most easily-observed examples of radiation hydrodynamics. Boundaries where fully-ionized H II regions transition to neutral/molecular photodissociation regions (PDRs) are of particular interest because marked temperature and density contrasts across the boundaries lead to evaporative flows and fluid dynamical instabilities that can evolve into spectacular pillar-like structures. When detached from their parent clouds, pillars become ionized globules that often harbor one or more young stars. H_2 molecules at the interface between a PDR and an H II region absorb ultraviolet light from massive stars, and the resulting fluoresced infrared emission lines are an ideal way to trace this boundary independent of obscuring dust. This paper presents H_2 images of four regions of massive star formation that illustrate different types of PDR boundaries. The Ara OB1 star formation region contains a striking long wall that has several wavy structures which are present in H_2, but the emission is not particularly bright because the ambient UV fluxes are relatively low. In contrast, the Carina star formation region shows strong H_2 fluorescence both along curved walls and at the edges of spectacular pillars that in some cases have become detached from their parent clouds. The less-spectacular but more well-known Eagle Nebula has two regions that have strong fluorescence in addition to its pillars. While somewhat older than the other regions, Cyg OB2 has the highest number of massive stars of the regions surveyed and contains many isolated, fluoresced globules that have head–tail morphologies which point towards the sources of ionizing radiation. These images provide a collection of potential astrophysical analogs that may relate to ablated interfaces observed in laser experiments of radiation hydrodynamics.

1. Introduction

Star formation is a complex dynamical process where the attractive force of gravity must overcome the dispersive effects of pressure and angular momentum. Once stars form, they provide feedback into the nascent molecular clouds by generating powerful bipolar outflows that evacuate cavities and deposit momentum into the clouds (see, e.g., [1]). In regions of star formation where the most massive star has a spectral type earlier than ~B3 ($M \gtrsim 10 M_\odot$), radiation is the primary feedback mechanism. In these cases, intense ultraviolet radiation from the massive stars ionizes an 'H II region' within which H is nearly fully-ionized. At the boundaries of an H II region, H quickly transitions to a high-density neutral state called a photodissociation region or PDR. Radiation that is less-energetic than the ionization potential of H (13.6 eV) penetrates into the PDR, and affects molecular chemistry by dissociating molecules, heating dust grains, and ionizing elements such as C [2].

Irradiated PDR interfaces are important to understand because it is here where radiation deposits energy into and ultimately disrupts the molecular cloud. The disruption occurs as neutral material at the front becomes ionized and, finding itself at a high temperature, ablates into the less-dense H II region. The ablation flow drives pressure waves and weak shock fronts back into the molecular cloud, heating the gas and dust near the interface and thereby enhancing the formation rate of complex molecules in the PDR. The ablation process may also affect star formation because gas located at the tips of pillars compresses in response to the radiation pressure. Some studies suggest this inward pressure may trigger stars to form at these locations, though it can be difficult to

* Corresponding author. Rice University, Physics and Astronomy, Houston, TX, USA.
E-mail address: hartigan@sparky.rice.edu (P. Hartigan).

1574-1818
http://dx.doi.org/10.1016/j.hedp.2012.08.002

distinguish sequential star formation, where there are simply spatial gradients in the apparent ages, from triggering [3]. The morphologies of the interfaces provide unique opportunities to study how fluid dynamical instabilities form and develop in astrophysical systems.

Hence, along with gravity and rotation, radiation hydrodynamics is one of the dominant physical processes in regions of massive star formation, and one that is amenable to study in the laboratory. The intense radiation environments present in laser experiments often produce ablation flows at locations where the radiation interacts with a surface [4]. As material ablates, the interfaces can become irregular in shape and eventually transform into pillar-like structures [5,6] whose morphologies resemble those present in molecular clouds subject to radiation from nearby massive stars [7].

H II regions and molecular clouds are distinct phases of the interstellar medium, and the clouds often show sharp boundaries that are easily-observed at optical wavelengths because dust within molecular clouds absorbs optical light from background sources such as stars or emission from the hot gas in the H II region. While these boundaries often exhibit beautiful and complex morphologies, connecting the observed morphologies with radiation-driven instabilities is not always a straightforward task. Depending on the situation, other physical processes such as bulk motions of molecular clouds relative to the gas within an H II region, internal magnetic and thermal pressure gradients, and the presence of dense clumps within clouds may be more important than radiation in determining how an interface appears and how it evolves with time.

To identify an interface as a promising analog for radiative-driven instabilites we need to separate regions where the ultraviolet flux is highest from others where the radiative flux is lower. From an observational standpoint, it is challenging to determine exactly where the ultraviolet radiation deposits its energy, because regions of star formation are so dusty that lines of sight to PDR interfaces are typically opaque at both optical and ultraviolet wavelengths. Hence, some of the apparent boundaries may simply result from a dense dusty cloud in the foreground that obscures a bright background H II region. Fortunately, because fluorescent ultraviolet excitation of H_2 is always accompanied by specific infrared emission lines that radiate as the molecule decays to its ground state, one can image true PDR interfaces directly in these infrared lines where obscuration by dust is negligible.

As a broad cut, one can sort massive star forming regions by the number of O stars, which, along with the rare luminous blue variable (LBV) and Wolf–Rayet (WR) stars, represent the classes of the most massive stars. The O-spectral class is subdivided by increasing mass and photospheric temperature into O9, O8, O7, and so on, up to about O3 and O2, which are the most massive O stars known. Less-massive stars are always more common, so, for example, a region that contains an O3 star will typically have many O5–O9 stars. The most massive stars should become supernovae within a few million years of their birth, and undoubtedly influence the ongoing star formation in their vicinity, which would otherwise last for tens of millions of years. While they are present, the UV radiation from the most massive stars will dominate the ionization of its surroundings because the most massive stars have the hottest photospheres and therefore the highest photon luminosities >13.6 eV. The UV luminosity (photons/second) depends strongly upon the photospheric temperature because the UV part of stellar spectra lies on the Wien portion of the blackbody curve. For example, a typical O3 star emits an order of magnitude more photons capable of ionizing H than does an O7.5 star, and nearly two orders of magnitude more than an O9.5 star [8].

This paper presents near-IR images of the PDR interfaces of four regions of massive star formation that span a range of ultraviolet radiation fields and morphologies, from large wall-like structures in a region with only a few O stars (Ara OB1), to spectacular pillars within more massive regions (Carina and Eagle), to isolated globules in an extremely massive and somewhat older complex (Cygnus OB2). The goal is to provide the laboratory astrophysics community with several examples of typical ablation interfaces that are present within regions of massive star formation, as these may prove to be useful analogs for ongoing or planned experimental work. The next section describes the physics of H_2 fluorescence along with the observational program, and the paper continues with a description of what the new images show in each of the four regions.

2. Infrared observations of fluorescent H_2

Fig. 1 summarizes the physics of fluorescent excitation of H_2. Ultraviolet photons with energies less than the ionization potential of H (13.6 eV) penetrate into the region of neutral gas where molecular hydrogen exists. If their energy is greater than about 10 eV, these photons can excite H_2 from its ground electronic state to the Lyman and Werner bands. These bands can be visualized as resulting from the overlap of the $n = 2$ levels of the indivdual H atoms atoms when the protons are separated by the intranuclear distance of ~1Å [9]. As excited H_2 molecules cascade back to their ground states, there is a probability that they will pass through the $J = 3$ (rotational) $v = 1$ (vibrational) level. Because H_2 is a symmetric molecule, it has no dipole moment, and transitions of $\Delta J = \pm 1$ do not occur. However, the molecule can decay via $\Delta J = -2$ quadrupole radiation to the $J = 1$ $v = 0$ level by emitting an infrared photon at 2.12 μm. Designated as the 1-0S(1) transition (S indicating $\Delta J = -2$ and '1' referring to the J-value of the lower state), this emission line traces the interface where the ultraviolet radiation encounters molecular hydrogen.

Our H_2 observations were taken with the NOAO NEWFIRM camera on two observing runs, 20–22 Sept 2008 at the 4-m telescope at Kitt-Peak National Observatory in Arizona, and at the 4-m telescope at the Cerro–Tololo InterAmerican Observatory (CTIO) in Chile 16–18 March 2011. A single NEWFIRM image has a large field of view of ~28 arcminutes, and a fine plate scale of 0.4 arcseconds per pixel. The seeing ranged between 0.7 and 1.8 arcseconds over the course of the observations with the exception of the H_2 and K-band images of M 16 (see Section 3.3). The final images have a spatial resolution ~4 times better than that possible with the Spitzer Space Telescope. In addition, unlike Spitzer observations of H_2 that rely upon broadband filters that transmit many emission lines as well as a large amount of continuum, the NEWFIRM H_2 observations were taken through a narrowband filter ($\delta\lambda/\lambda \sim 1\%$) centered on the 1-0S(1) 2.12 μm transition. As part of the program we sometimes also obtained a narrowband 2.16 μm Brγ image to detect recombination from H in the H II region and to aid in continuum subtraction, and a broadband 2.2 μm K-image to identify continuum from warm dust. A typical observing sequence involved a grid of up to 72 images dithered spatially in a set pattern. Data reduction followed a procedure more fully-described elsewhere (10).

Infrared observations of the southern targets (Ara, Eagle and Carina) were complemented by broadband optical B, V, R, and I and narrowband Hα images taken with the Y4KCam at the CTIO 1-m YALO telescope 12–17 March 2011. The Y4KCam is a 4064 × 4064 backside-illuminated CCD with a plate scale of 0.289 arcseconds per pixel and a field of view of 20 arcminutes. Data reduction followed standard bias-subtraction and flatfielding procedures, with the additional requirement that twilight sky flats were needed to remove a residual large-scale illumination pattern. Several position

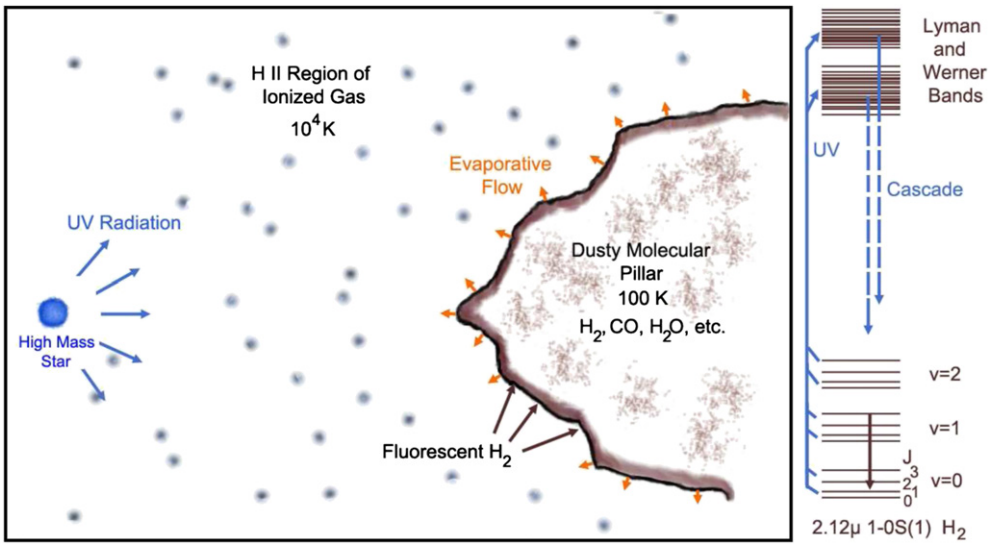

Fig. 1. Schematic of an H II/photodissociation region and its fluorescent H_2. Ultraviolet light from the massive star excites H_2 to the Lyman and Werner bands. The 2.12 μm emission line radiates as H_2 molecules cascade down to their lower states. Infrared lines like 2.12 μm penetrate through intervening dust, which absorbs ultraviolet and optical light, and as such are ideal tracers of the interface between the ionized and molecular gas when the ultraviolet radiation field is strong.

dithers were used for each image to reduce internal reflections from bright stars in the final median composite. We used a distortion map determined from stellar positions to align the Y4KCam images with the NEWFIRM data to within ∼0.1 arcseconds. All data reductions were performed within the IRAF environment.

The narrowband H_2 filter blocks most of the continuum present in the K-band, but all filters admit some continuum. It can be important to remove this component when comparing the spatial positions of different emission lines along an interface, and in regions where there are many background stars. However, the continuum does not affect appearance of the PDR boundaries in the images significantly because the H_2 bandpass is narrow enough that infrared continuum contributions are small in the target objects. Subtracting a scaled K-band image to remove continuum can be problematic owing to slightly differing seeing conditions and sub-pixel alignment differences. For these reasons the narrowband images are uncorrected for continuum, though we make use of the K-band to help interpret the regions, and in some cases subtract the continuum with a scaled Brγ or K-band image to create an image that removes most stars and highlights the PDR interfaces.

3. H_2 images of PDR interfaces

3.1. Ara OB1

Ara OB1 is a region of star formation in the southern sky centered ∼1.5° out of the galactic plane and subtending about a degree on the sky (∼20 pc at its distance of 1320 pc, [11],). Its stellar population consists of a young open cluster, NGC 6193, whose most massive members are an O7 star and an O5/O6 binary [12], similar to the situation in the Orion Nebula. Ultraviolet radiation from these stars illuminates the Rim Nebula NGC 6188, a delicate undulating feature located about 15 arcminutes (6 pc) to the west of the cluster. The Rim Nebula outlines the edge of a dark cloud, within which lies an embedded star formation region known as RCW 108. A CO survey of the region uncovered many distinct clouds along the line of sight [13].

New Hα, Brγ, and H_2 images of the region are shown in Fig. 2. The Hα image highlights material as it boils off the PDR and recombines as it becomes ionized. Although the Hα image outlines the interface between the ionized and neutral gas well, the boundary is not sharp and is strongly affected by dust extinction. The multicolor composite in the middle panel shows a thin red (H_2) feature which marks the actual boundary of the PDR where the UV light is absorbed. This boundary is also clear in the difference image (Brγ−H_2) in the right panel. The advantage of the difference image is that Brγ and H_2 1-0S(1) have nearly the same wavelength, so the relative amount of stellar continuum for each star is nearly the same for all sources, and as a result the stars tend to subtract out. The H_2 feature circled in the right panel has a more clumpy morphology and appears to originate from the RCW 108 region. This feature may be a stellar jet that becomes visible as shock waves heat the ambient H_2. If it is a jet, the H_2 knots should exhibit detectable proper motions on the sky after a suitable time interval.

Overall, the Rim Nebula is a wonderful example of an interface that appears more or less linear on the sky, and exhibits the beginnings of pillar formation. Two features at the top of the H_2 image and one at the bottom are ∼0.5 pc in size, with many smaller features present along the rim, though there is a lack of detached irradiated globules. The ultraviolet radiation field in Ara OB1 is not particularly strong because the hottest star is only an O5, and this results in a detectable, albeit moderate signal of H_2 from the PDR interface. As in all such regions, without a dedicated numerical study one cannot readily determine if the undulating structure present along the Rim Nebula results from variations in the gas density along the rim, from instabilities induced by radiation, or some combination of the two.

3.2. Carina

The star formation region in Carina is the premier example of its kind in the southern sky. The region has ∼70 O stars, more than any other OB association in the southern sky within 3.5 kpc, and excites a large H II region and nebula that is visible to the naked eye. Its most famous resident is undoubtedly η Car, a luminous blue variable (LBV) that was once one of the brightest stars in the sky before it ejected a massive shell about 170 years ago [14], and is a prime candidate for the next supernova in our galaxy. Several clusters of massive stars, including Tr 14, Tr 15, Tr 16, Bo 10, Bo 11, Coll 228, and

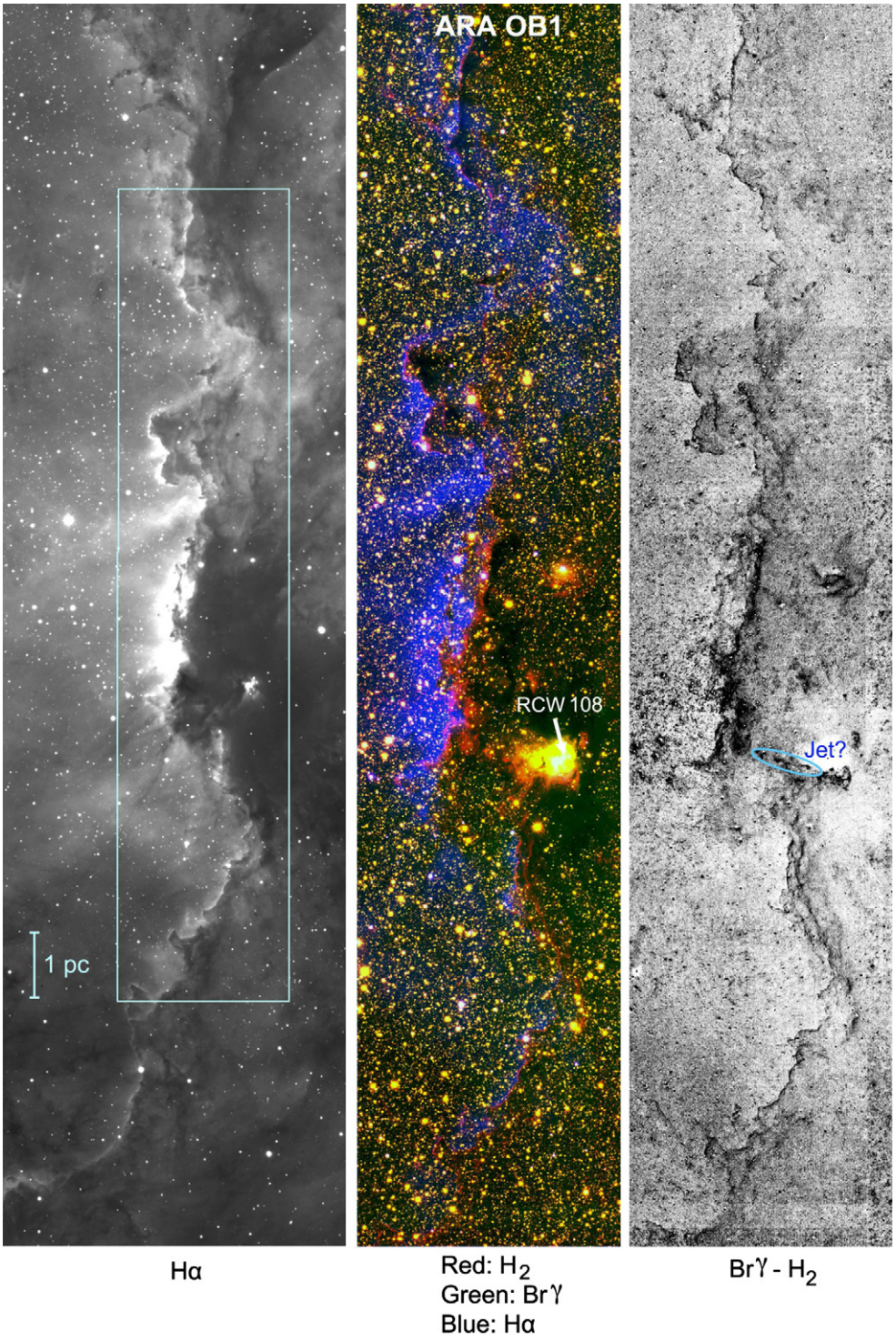

Fig. 2. Images of the Ara OB1 star formation region (standard convention of north up and east to the left). Left: this narrowband Hα image highlights recombining H gas as it boils off the dark cloud. The cyan box shows the area covered in the center and right panels. The scale bar assumes a distance of 1320 pc. Center: color composite of the region showing the Hα emission (blue) as it expands away from the PDR interface (H_2, shown in red). A large number of background and embedded stars appear yellow in the composite because they are only present in the infrared (H_2, in red, and Brγ in green) images. The embedded star formation region RCW 108 is marked. Right: subtraction image, where H_2 emission appears black and Brγ emission white. Stars tend to subtract out in this image, which shows the boundary of the PDR in H_2. (For interpretation of the references to color in this figure legend, the reader is referred to the web version of this article.)

Coll 232 exist in the vicinity. The distance to the region is uncertain owing to difficulties in accounting for reddening [15]; a recent study found 2.9 kpc to both Tr 14 and Tr 16 [16], so we will adopt this value. Carina is home to a number of O2 and O3 stars [8], and ages for the stellar content range from 0 to 5 Myr [15].

The UV radiation field in Carina is dominated by two clusters. The first, Tr 16, is a loose grouping that spreads out over ∼8 pc. It contains 42 O stars in all, a WR star, η Car, three O3 stars, and shows evidence for subclustering [17]. The second cluster, Tr 14, is much more compact, and contains ten O stars, including an O2 star and an

O3.5 star [8,15]. Tr 16 is situated about a parsec in projection south of η, some 10 pc to the southeast of Tr 14. Optical images of the center of Car OB1 from HST and from the ground provide a snapshot of the harsh, chaotic environment that surrounds a region of massive star formation like Carina once the strong UV radiation and winds from the nearby O and B stars begin to clear away the molecular clouds in their vicinity. These images reveal a wealth of flows, globules, and star formation activity in the region [18].

A full report of our Carina observations will appear elsewhere [10], but Fig. 3 provides a sample of the sort of PDR structures that are present in the region. The color composite illustrates a striking transition between the highly-ionized [O III] emission (blue) to the recombination lines of H (Brγ, green), to the fluoresced H_2 line emission (red) as one proceeds into the molecular cloud. By magnifying the bright PDR wall on the right side of the image, we see that the H_2 emission appears highly filamentary and fragmented, and includes many ragged-shaped pillars. Other large-scale wavy wall-like structures are shown in panels B and G. Panel G overlaps with the top right corner of panel A, and the cloud there is probably illuminated mainly by Tr 14. The object in panel B appears to have a star near its apex, with a bright rim on its northwest side. Multiple exciting sources may play a role here, as

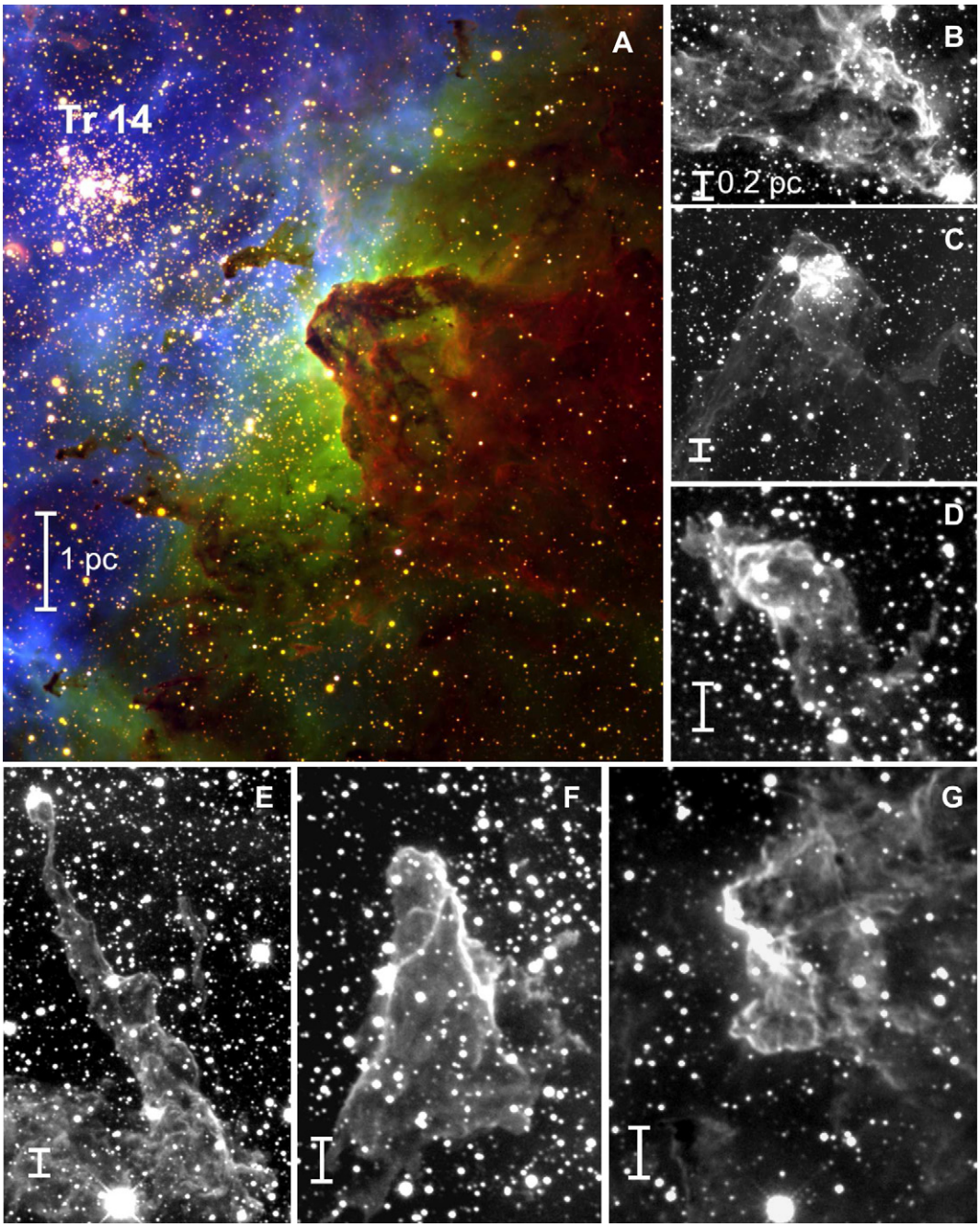

Fig. 3. Images of selected portions of the Carina star formation region. The color composite has [O III] 5007Å in blue, Brγ in green and H_2 1-0S(1) in red. The compact cluster of O stars Tr 14 is marked. The other panels are greyscale images of H_2 at various locations throughout the region. Carina has spectacular pillars, walls, and proplyds. Scale bars assume a distance of 2.9 kpc, and are 0.2 pc in all panels except for the color composite. Each panel is discussed in the text. (For interpretation of the references to color in this figure legend, the reader is referred to the web version of this article.)

both Tr 16 and Tr 14 are located to the northwest, with distances of 8.0 pc and 18.0 pc, respectively, to η Car and to the center of Tr 14.

Panel C displays a small young cluster that has formed within a globule. The globule is irradiated by sources to the north, which may include stars in both Tr 16 (center $\sim$13 pc away) and Tr 14 (24 pc away), but the cluster has also created its own PDR along a cavity wall within the globule on its northeast side. Spectacular irradiated pillars (E and F) and more complex structures (D) are located in the same general area as the object in panel C and also respond to UV radiation from sources to the north.

It is clear that Carina is a very rich environment where one can study how molecular clouds transform when they are subjected to intense UV radiation fields and strong stellar winds. Structures of all types abound here, including many varieties of walls, pillars, and detached globules. In response to the UV fluxes, the fluoresced H_2 emission is quite bright, even along the sides of the pillars. One challenge with interpreting the region is that many possible ionizing sources exist and the radiation does not necessarily mainly come from a single direction.

3.3. Eagle Nebula

The Eagle Nebula (M 16) is instantly recognizable to the public because of the so-called 'Pillars of Creation' images published during the early days of the Hubble Space Telescope [19], and subsequent images of the 'Spire' taken as part of the Hubble Heritage project. The Pillars have been studied in molecular line emission [20], and recent space-based surveys include Spitzer observations in the near-infrared [21] and Herschel observations in the mid- and far-infrared [22]. In a study of the Pillars with a Fabry-Perot, Allen et al. observed H_2 near the apices of the Pillars, and found this emission to be offset from Brγ in the direction away from the ionizing sources [23]. The sharpest images of the Pillars in the H_2 and Brγ lines come from the NICMOS camera on HST [24], and show this spatial offset clearly, along with exquisite detail of the H_2 that resembles the structured filaments we observe in Carina (Fig. 3). However, the very small field of view of NICMOS limited these observations to the immediate area around the heads of the Pillars.

Using a distance to the Eagle of 1.8 kpc [25], the Pillars and the Spire are located $\sim$2 pc to the southeast and east, respectively, of a dense open cluster of stars known as NGC 6611. This cluster contains about a dozen O stars, with the most massive being an O4 [26]. NGC 6611 has ejected several lower-mass O stars that form bow shocks as they move through the interstellar medium [27]. The M 16 area has ongoing star formation, with typical ages of a few million years for the young stars [3,28]. North of the cluster, the Herschel and Spitzer images show what appears to be the ridge of a dark cloud, and a fainter arch that extends further to the north [21,22]. Based on the count of O-stars, the Eagle Nebula falls somewhere between Ara OB1 and Carina on the scale of massive star formation.

Our observations of the Eagle appear in Fig. 4. The H2 images were taken in poor seeing conditions (2.8 arcseconds, as compared to 0.8 arcseconds for Brγ) which has the effect of blurring out sharp features. Nonetheless one can identify that the main interaction regions are the Pillars, the Spire, and the Ridge, with the most extensive H_2 located in the Ridge. Spatial offsets between the Brγ and H_2 are in the same sense that we observed in Ara and Carina, with the Brγ emission located closer to the ionizing sources in the cluster. The cluster appears particularly dense in the infrared (lower left portion of the Ridge image). At the southern edge of the North Bay, a dark feature visible at optical wavelengths, we observe knots of H_2 emission that may represent a molecular jet. The Spitzer IRAC image at 8 μm also shows this feature, albeit with rather poor spatial resolution [21].

Despite the notoriety of its famous pillars, the Eagle Nebula is only a modest hunting ground for irradiated interfaces. As Thompson et al. note [24], much of the star formation activity may be finished in the Eagle, leaving only a few areas like the Ridge and the Pillars for irradiated interfaces. Apart from the possible jet at the bottom of the North Bay, our H_2 images do not reveal any striking new features, though in addition to the well-known Pillars and Spire, we can identify the Ridge as a promising area where extensive, and relatively bright PDR interfaces exist. Images of the Ridge taken during better seeing conditions would likely resolve the H_2 emission into a filamentary, bumpy wall like we observed in Ara OB1.

3.4. Cygnus OB2

If one were to fly far above the galactic plane and look down upon the structure of the Milky Way within a few kpc of the Sun, a single star formation region would stand out as being the major area of activity in this portion of the galaxy: Cyg OB2. Also known as Cygnus X, the region houses over 120 O stars, including several of type O3 [29], has a candidate for the most massive star in the galaxy, evidence for recent supernovae [30], and may even be the source of a large-scale galactic fountain [31]. The region would be a naked-eye cluster known to all amateur astronomers were it not for the fact that it lies near the galactic plane along the Cygnus arm, and for that reason suffers 10 magnitudes of visual extinction along the line of sight. X-ray observations reveal at least a thousand young stars in the region [32].

The new H_2 observations cover an area over 1.5° on a side, and include the entire star-forming region. Fig. 5 depicts some of the more interesting of these structures. A dense cluster of massive stars anchored by the O3 star S 22 at the core of the region (panel D) is the main source of radiation, although O stars are scattered throughout the area. Surrounding the core we find dozens of irradiated globules that possess head–tail structures with the tails pointing away from the ionizing sources. Several of these are shown in Fig. 5, along with an arrow that denotes the distance to S 22. Some of these objects have been discovered independently by other authors and described in recent papers [33,34].

Each panel demonstrates an important aspect of radiation hydrodynamics in the star formation process. Panel A shows that two stars within this globule are surrounded by reflection nebulae, indicating that stars still form here. Narrow filaments of H_2 are associated with the stars in the globule as they create their own cavity from an outflowing wind, but the overall shape of the PDR is still driven by the cluster of O stars at the large projected distance of over 20 pc. Hence, young massive stars like those in Cyg OB2 can influence the ongoing star formation over a very large volume. This motif repeats in panel C, where a young star at the apex of the globule appears to have created enough of a cavity to nearly detach from its globule. Panel B depicts what appears to be an earlier stage reminiscent of the wall in Ara OB1, where small pillars are beginning to form.

Panels E and F display small remnants of globules that appear similar to objects known as proplyds in the Orion Nebula. The proplyd within panel E possesses a wonderful 'wiggling' tail that resembles a Kelvin–Helmholtz instability (see also [33]). However, it is unclear what role stellar winds from the core play in creating this shape, as the wind should first encounter a strong bow shock around the obstacle before the postshock wind could interact with the neutral material to create a shear layer that would induce mass stripping. The H_2 images here show only the boundary where the molecular gas becomes excited by direct UV radiation from the core stars and by ambient UV radiation scattered within the H II region or originating from less massive O stars in the vicinity. It is likely

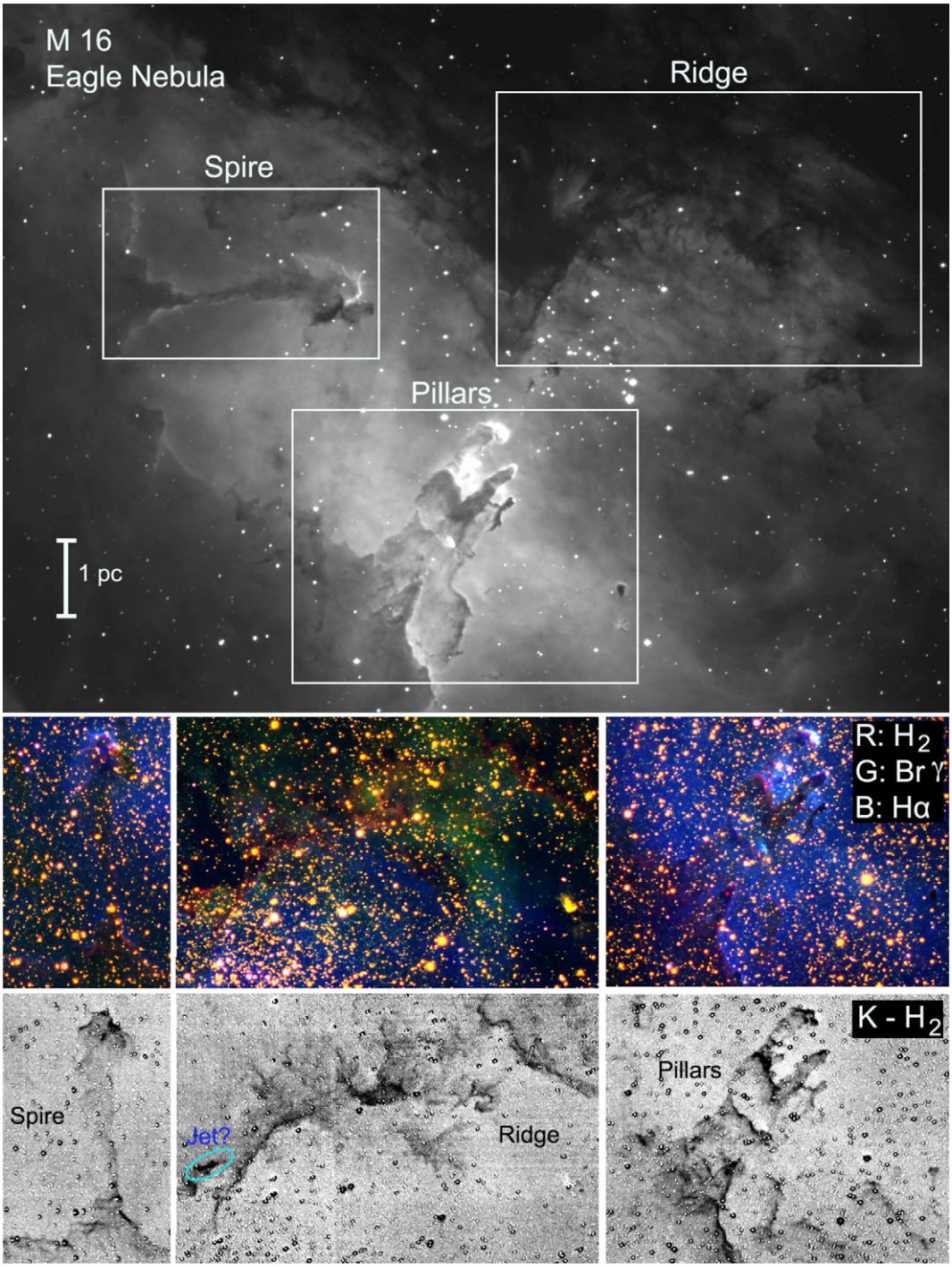

Fig. 4. Images of the Eagle Nebula. Top: Hα image, showing the locations of the spire, ridge, and pillars that are magnified in the subsequent panels. The North Bay is the dark region along the left of the ridge image. Middle: color composites of the magnified regions, with Hα in blue, Brγ in green, and H_2 1-0S(1) in red. Bottom: difference between a continuum band (K) and a narrowband H_2 image, highlighting the PDR boundaries. The scale bar assumes a distance of 1.8 kpc. (For interpretation of the references to color in this figure legend, the reader is referred to the web version of this article.)

that a bow shock is present ahead of the proplyd, but this shock would be difficult to detect if the wind from the massive stars is fully ionized. The wave-like structure along the sides of the proplyd in panel E has a characteristic length on the order of the size of the dense clump at the head of the globule. Panel F shows similar structures, but not all of these have formed a star at their apices.

The Cyg OB2 region is among the most massive star formation regions in our galaxy. The many O stars scattered throughout the region and the lack of bright irradiated walls near the cluster suggests may be several million years older than our other targets [35], though some star formation continues within the few remaining globules. These globules, probably the densest leftovers from the original molecular cloud, glow along their boundaries in H_2 as they respond to the intense UV ambient radiation field and possibly strong stellar winds from O stars in the area. In some cases radiation from one or more young stars at the head of the globule

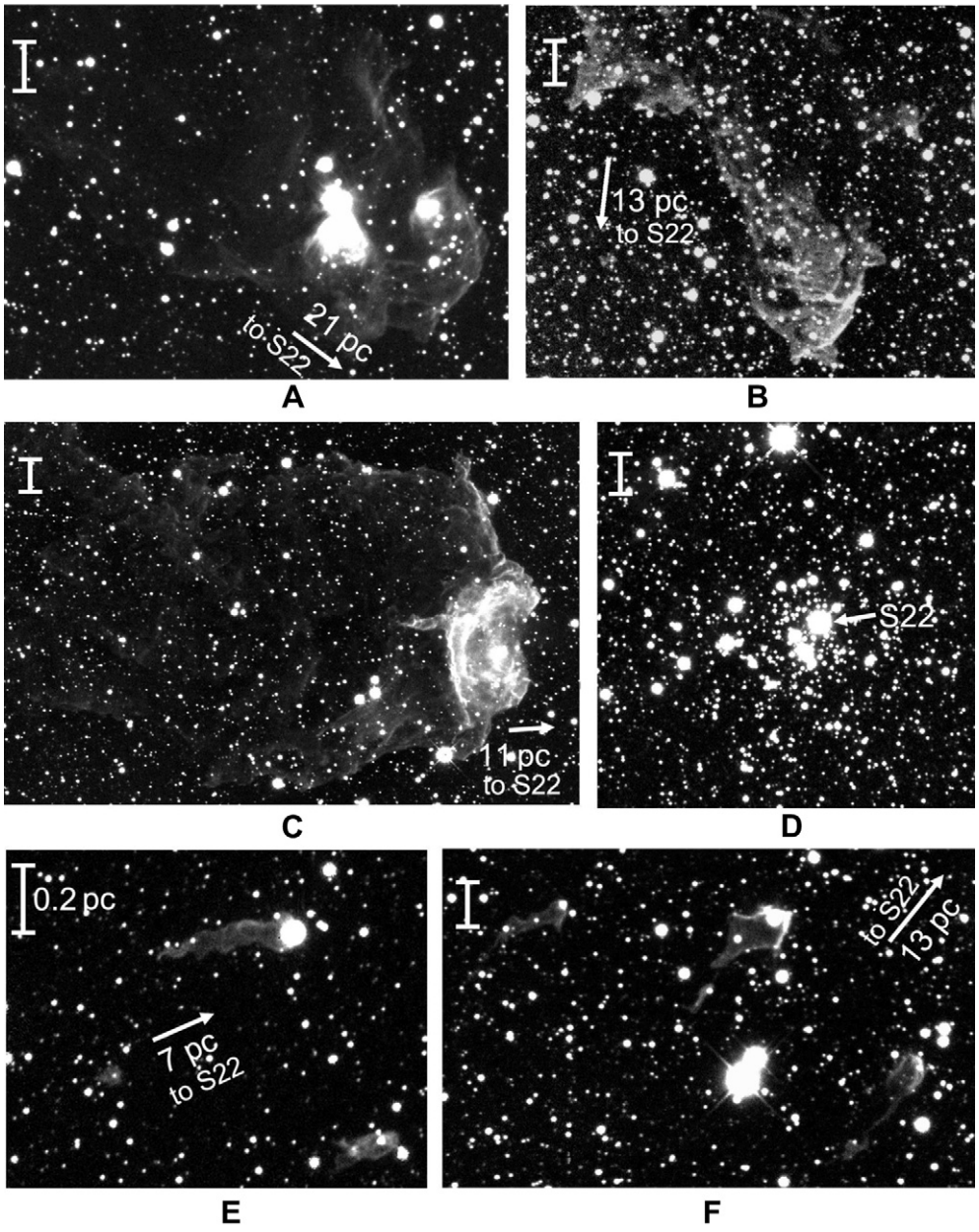

Fig. 5. H_2 images of globules in the Cyg OB2 star formation region. The brightest O star in the central cluster, Schulte 22, is labeled in panel D and forms the nominal center of the region. Arrows in each panel indicate the distance (from the base of the arrow) and direction to S 22. Objects within each of the panels are discussed in the text. North is up and east to the left, and the scale bars are 0.2 pc for each panel, and assume a distance of 1.7 kpc to the system.

also affects the dynamics of the system. In Cyg OB2 we are witnessing the last stages of the photoablation processes in a region where the most massive stars have already formed and have cleared away most of the ambient material.

4. Summary

Regions of massive star formation offer some of the best and most easily-observed examples of radiation hydrodynamics. The boundary where the fully ionized H II region transitions to the neutral/molecular photodissociation region is of particular interest because the marked temperature and density contrasts across the boundary lead to evaporative flows and fluid dynamical instabilities that can develop into spectacular pillar-like structures. Pillars subsequently become ionized globules when they detach from their parent clouds, and the globules often harbor one or more young stars at their apices. It is possible to observe the interface between the H II region and PDR directly by imaging in the light of the H_2 1-0S(1) transition, which occurs as a byproduct of fluorescent excitation of H_2 to the Lyman and Werner bands. Extinction by dust is negligible at 2.12 μm, so it is possible to observe this interface directly, and with better spatial resolution than was possible from wide-field space-based missions such as Spitzer and Herschel.

The new images illustrate how radiation can sculpt molecular clouds into a variety of spectacular forms. Notwithstanding the dizzying array of morphologies, there appears to be a progression from (i) the wavy wall-like structure in Ara OB1, where radiation appears to have had as yet only a modest influence on the molecular cloud, to (ii) the intricate pillars and cavity walls within Carina and to a lesser extent in the Eagle Nebula, where radiation and outflows are in the process of tearing the cloud apart, to (iii) the relatively isolated head-tail globules in Cygnus OB2, where the

massive stars have already dissipated much of the natal molecular cloud, and leave behind only small remnants.

Future efforts by our group will focus on quantifying how spatial offsets between different emission lines in the PDR change as the ultraviolet radiation source varies in strength. Finding evidence for or against stellar wind shocks is another important observational goal, as the massive stars which generate the UV radiation field can also drive powerful winds that disrupt their surroundings. Numerically, there is a clear challenge to predict offsets between different emission lines in a PDR, and to distinguish irregular interfaces where the shape is driven by radiative instabilities from those produced by dense clumps within the molecular cloud. Combining radiation with winds should be another numerical frontier. On the experimental side, new programs at Omega and NIF should begin to explore the regime of radiative shocks and strongly-irradiated interfaces [36–38], and can look for similar structures to the ones presented here.

Acknowledgements

This work was made possible through DOE funding via the NLUF program. We thank R. Probst for his assistance with the KPNO observations, the staff of CTIO for their support at the 4-m and 1-m telescopes and W. Henney for useful discussions about PDRs.

References

[1] H. Zinnecker, H.W. Yorke, Annu. Rev. Astron. Astrophys. 45 (2007) 481.
[2] D.J. Hollenbach, A.G.G.M. Tielens, Rev. Mod. Phys. 71 (1999) 173.
[3] M.G. Guarcello, G. Micela, G. Peres, L. Prisinzano, S. Sciortino, Astron. Astrophys. 521 (2010) A61.
[4] Kuranz, C.C., HEDP, in press.
[5] A. Mizuta, J.O. Kane, M.W. Pound, B.A. Remington, D.D. Ryutov, H. Takabe, Astrophys. J. 647 (2006) 1151.
[6] D.D. Ryutov, J.O. Kane, A. Mizuta, M.W. Pound, B.A. Remington, Astrophys. Space Sci. 307 (2007) 173.
[7] M.W. Pound, J.O. Kane, D.D. Ryutov, B.A. Remington, A. Mizuta, Astrophys. Space Sci. 307 (2007) 187.
[8] N. Smith, MNRAS 367 (2006) 763.
[9] G. Herzberg, Molecular Spectra and Molecular Structure I. Spectra of Diatomic Molecules, Van Nostrand Reinhold, New York, 1950.
[10] Hartigan, P. et al., in preparation.
[11] W. Herbst, R.J. Havlan, Astron. Astrophys. 30 (1977) 279.
[12] E.M. Arnal, N.I. Morrel, B. Garcia, O.H. Levato, PASP 100 (1988) 1076.
[13] E.M. Arnal, J. May, G.A. Romero, Astron. Astrophys. 412 (2003) 431.
[14] N. Smith, D.J. Frew, MNRAS 415 (2011) 2009.
[15] J. Ascenso, J. Alves, S. Vicente, M.T.V.T. Lago, Astron. Astrophys. 476 (2007) 199.
[16] H. Hur, H. Sung, M.S. Bessell, Astrophys. J. 143 (2012) 41.
[17] S.J. Wolk, et al., Astrophys. J. 194 (2011) 11.
[18] N. Smith, J. Bally, N.R. Walborn, MNRAS 405 (2010) 1153.
[19] J.J. Hester, et al., Astrophys. J. 111 (1996) 2349.
[20] M.W. Pound, Astrophys. J. 493 (1998) L113.
[21] R. Indebetouw, T.P. Robitaille, B.A. Whitney, E. Churchwell, B. Babler, M. Meade, C. Watson, M. Wolfire, Astrophys. J. 666 (2007) 321.
[22] T. Hill, et al., Astron. Astrophys. 542 (2012) A114.
[23] L.E. Allen, M.G. Burton, S.D. Ryder, M.C.B. Ashley, J.W.V. Storey, MNRAS 304 (1999) 98.
[24] R.I. Thompson, B.A. Smith, J.J. Hester, Astrophys. J. 570 (2002) 749.
[25] C. Bonatto, J.F.C. Santos, E. Bica, Astron. Astrophys. 445 (2006) 567.
[26] M.G. Guarcello, M. Caramazza, G. Micela, S. Sciortino, J.J. Drake, L. Prisinzano, Astrophys. J. 753 (2012) 117.
[27] V.V. Gvaramadze, D.J. Bomans, Astron. Astrophys. 490 (2008) 1071.
[28] L. Hillenbrand, P. Massey, S. Strom, K. Merrill, Astrophys. J. 106 (1993) 1906.
[29] P. Massey, A.B. Thompson, Astrophys. J. 101 (1991) 1408.
[30] W. Bednarek, MNRAS 382 (2007) 367.
[31] D.C. Abbott, J.H. Bieging, E. Churchwell, Astrophys. J. 250 (1981) 645.
[32] J.F. Albacete Columbo, E. Flaccomio, G. Micela, S. Sciortino, F. Damiani, Astron. Astrophys. 464 (2007) 211.
[33] R. Sahai, M.R. Morris, M.J. Claussen, Astrophys. J. 751 (2012) 69.
[34] N.J. Wright, J.J. Drake, J.E. Drew, M.G. Guarcello, R.A. Gutermuth, J.L. Hora, E. Kraemer, Astrophys. J. 746 (2012) L21.
[35] F. Comeron, A. Pasquali, F. Figueras, J. Torra, Astron. Astrophys. 486 (2008) 453.
[36] Casner, A. et al., HEDP, in press.
[37] C.C. Kuranz, et al., Astrophys. Space Sci. 336 (2011) 207.
[38] Trantham, M. et al., in press.